Materials Science & Engineering A 613 (2014) 141–147

Contents lists available at ScienceDirect

Materials Science & Engineering A

journal homepage: www.elsevier.com/locate/msea

Flow behavior and processing maps of 2099 alloy

F. Zhang [a,b,*], J.L. Sun [b], J. Shen [a], X.D. Yan [a], J. Chen [a]

[a] Nonferrous Metals Processing Division, General Research Institute for Nonferrous Metals, Beijing 100088, China
[b] School of Materials Science and Engineering, University of Science and Technology Beijing, Beijing 100083, China

ARTICLE INFO

Article history:
Received 6 May 2014
Accepted 23 June 2014
Available online 30 June 2014

Keywords:
2099 alloy
Flow behavior
Processing maps
DRV
DRX

ABSTRACT

The flow behavior of 2099 alloy was investigated by means of hot compression tests in the temperature range of 300–500 °C and strain rate range of 0.001–10 s^{-1}. Processing maps were developed on the basis of the dynamic materials model (DMM). The results show that the flow stress increases with increasing strain rate and decreasing temperature. At a given deformation condition, the flow stress composed three stages: work hardening stage, softening stage and steady stage. Microstructure observation indicates that in the deformation temperature range of 300–420 °C and strain rate of 0.001–10 s^{-1} shows a dynamic recovery (DRV) character; while that deformed in the deformation temperature range of 420–500 °C and strain rate of 0.001–10 s^{-1} shows a dynamic recrystallization (DRX) character. According to the processing map and microstructure observation, DRV and DRX are the main deformation mechanisms in the safe regions, while flow instability is manifested as adiabatic shear bands and flow localization at the strain of 0.7. The optimum processing parameters for 2099 alloy at different strains conditions are given with the efficiency dissipation more than 0.3.

1. Introduction

The high stiffness to density ratio and strength to weight ratio, excellent fatigue resistance and cryogenic toughness properties of Al–Li alloys make them potential replacement for traditional 2xxx and 7xxx series aluminum alloys in structural components of aerospace applications [1]. For every 1 wt% addition of Li to Al, the elastic modulus of Al increases by 6% and the density reduces by 3%, up to the maximum solid solubility of Li in Al, i.e. 4.2 wt% Li [2]. A representative 3rd generation Al–Li alloy is the 2099 alloy, which has been found to save up to 14% weight on major structural components of aircraft wings and 21% for some cryogenic tanks [3]. Heretofore, 2099 alloy has many applications in aerospace which is used in all applications from structures and plating to cryogenic containers [1,4,5]. In past few years, many researchers have paid attention to this alloy, especially in terms of its aging process and failure behaviors [6,7]. However, there is a lack of knowledge on the workability of 2099 alloy.

The workability of alloy refers to the plastic deformation ability that a metal can be deformed easily without fracture during bulk deformation process such as rolling, forging, extrusion, and rolling [8]. Workability can be evaluated by means of processing map, and constructed from experimentally generated flow stress variation with respect to strain, strain rate, and temperature. A processing map shows in the processing space, i.e. on the axes of temperature and strain rate, the processing conditions for stable and unstable workability deformation [9]. Processing maps have been proven to be a useful tool for the optimization of hot working processes for a wide range of metals and their alloys, or for the design of process parameters for new materials. By using the map, the deformation mechanisms in varied deformation conditions can be predicted, and the unstable deformation zones that should be avoided during hot deformation process can be received. Accordingly, the techniques can be optimized through the map, and it is easy to control the structures and properties, reduce the failure in deformation process, and increase the production quality and reliability [10]. This methodology has been used to optimize the hot workability of various materials, such as aluminum alloy [11,12], magnesium alloy [13,14], titanium alloy [15,16], and other materials [17,18].

In this paper, the processing maps at different strains are established based on the dynamic materials model (DDM), according to the corrected experiment data in the isothermal compression of 2099 alloy [19]. Coupling with the microstructure evolution, the processability of 2099 alloy is investigated through calculating the efficiency of dissipation and the instability parameter at different process parameters. The reasonable process parameters will provide the important guideline for the optimization of deformation techniques and the improvement of microstructure.

* Corresponding author at: Nonferrous Metals Processing Division, General Research Institute for Nonferrous Metals, Beijing 100088, China. Tel.: +8610 6177055 820; fax: +8610 61770571.
E-mail address: zffreefly@126.com (F. Zhang).

http://dx.doi.org/10.1016/j.msea.2014.06.085
0921-5093/

2. Dynamic materials model (DMM)

According to Prasad et al. [20], processing map represents the response of the material in terms of microstructure evolution for the imposed strain and strain rate during hot deformation, and comprises the superimposition of power dissipation map and instability map. The hot compression test results were employed to construct processing map based on DMM. The DMM model considers mechanical processing as a system and work-piece as a power dissipater. At any given strain and temperature, the total power P consists of two complementary parts: G represents the power dissipation through plastic deformation, most of which is converted into the viscoplastic heat, and J represents the power dissipation through microstructure transition, such as dynamic recovery (DRV), dynamic recrystallization (DRX), superplastic flow, phase transformations, as well as damage of the material [21]. During plastic flow, P is described as follows [22]:

$$P = G + J = \sigma\dot{\varepsilon} = \int_0^{\dot{\varepsilon}} \sigma \, d\dot{\varepsilon} + \int_0^{\sigma} \dot{\varepsilon} \, d\sigma \tag{1}$$

where σ is the flow stress (MPa) and $\dot{\varepsilon}$ is the strain rate (s^{-1}). In this phenomenological model, the contents G and J can be related by the parameter m (the strain rate sensitivity), which is given as follows [11]:

$$\left(\frac{\partial J}{\partial G}\right)_{\varepsilon,T} = \frac{\partial P}{\partial G}\frac{\partial J}{\partial P} = \frac{\sigma \, d\dot{\varepsilon}}{\dot{\varepsilon} \, d\sigma} = \left[\frac{\partial(\ln \sigma)}{\partial \ln(\dot{\varepsilon})}\right]_{\varepsilon,T} = m \tag{2}$$

For the given strain and deformation temperature, the flow stress can be expressed as [12]

$$\sigma = K\dot{\varepsilon}^m \tag{3}$$

At any deformation temperature and strain supplied, J can be gained by combining Eqs. (1) and (3) and is expressed by

$$J = \sigma\dot{\varepsilon} - \int_0^{\dot{\varepsilon}} \sigma \, d\dot{\varepsilon} = \frac{m}{m+1}\sigma\dot{\varepsilon} \tag{4}$$

For the ideal linear dissipating body, $m=1$ and $J = J_{max} = \sigma\dot{\varepsilon}/2 = P/2$, and the power dissipation capacity of the material can be evaluated by the efficiency of power dissipation, η, which is defined as follows [14]:

$$\eta = \frac{J}{J_{max}} = \frac{2m}{m+1} \tag{5}$$

With the change of deformation temperature and strain rate, η varies, which represents the characteristics of power dissipation through microstructure transition.

By utilizing the principle of the maximum rate of entropy production, a continuum criterion for the occurrence of flow instabilities is defined in terms of another dimensionless parameter, ξ [15]

$$\xi(\dot{\varepsilon}) = \frac{\partial \ln[m/(m+1)]}{\partial \ln \dot{\varepsilon}} + m \le 0 \tag{6}$$

The variation of the parameter with the deformation temperature and strain rate at a given stain constitutes the flow instability map, which denotes the flow instability in deformation at different deformation conditions. However, Narayana Murty et al. consider that the efficiency of power dissipation (η) given in Eq. (5) in terms of the strain rate sensitivity parameter (m) is only valid explicitly when the flow stress–strain rate curve obeys the power law, where m is independent on strain rate [23]. Otherwise, if m is dependent on strain rate, then Eq. (6) becomes erroneous. So they propose a simplified flow instability condition for any type of flow curves [24]

$$2m < \eta \text{ or } m < 0 \tag{7}$$

The instability region identified by Eq. (7) is larger than that identified by Eq. (6), which is consistent with the experiment results. The same conclusion is also obtained in other alloys and the criterion should be more appropriate for delineating the regions of unstable metal flow during hot deformation.

3. Experimental procedure

The chemical composition (wt%) of the 2099 alloy used in the test was as follows: Cu – 2.6, Li – 1.75, Zn – 0.64, Mg – 0.29, Mn – 0.3, Zr – 0.08, and Al – bar. The ingot with 540 mm in diameter and 3000 mm in length were was prepared via the ingot metallurgy method followed by a heat treatment at 515 °C for 18 h and 525 °C for 16 h. The specimens were cut from it with dimension of ∅ 10 mm × 15 mm, and two grooves of 0.2 mm in depth were machined into the end faces of each sample. Fig. 1 shows orientation imaging microscopy of 2099 alloy, the average grain size is about 479 μm. The specimens were compression deformed at the temperature range from 300 °C to 500 °C and the strain rate range from 0.001 s^{-1} to 10 s^{-1} on a Gleeble-1500 thermal-mechanical simulator. In order to reduce the deformed friction, a graphite lubricant was used between the specimens and the crossheads. All the tests were performed with a heating rate of 10 °C/s and held for 3 min to secure a stable and uniformity temperature prior to deformation. All specimens were deformed to the total true strain of about 0.7 and water-quenched from test temperature to preserve the microstructure. The load-stroke data were converted into true stress–strain curves using standard equations, and the flow stress–strain curves were obtained automatically.

Specimens after deformation were sectioned in the center parallel to the axis and the cut surface was mechanically polished using standard techniques and electrochemically polished in a solution containing 5 ml $HClO_4$ and 95 ml methanol at 20 V for 30 s at room temperature for EBSD investigation. TEM microstructure was investigated by JME-2100. The TEM films were prepared by the conventional method: mechanically ground to 0.05 mm, and two-jet thinning in a solution of 30% HNO_3 and 75% methanol, and then cooled to −20 °C.

4. Results and discussion

4.1. True stress–strain curves

The corrected (friction and temperature correction) true stress–strain curves of 2099 alloy under different conditions are depicted in Fig. 2. As is seen, the flow stress level is significantly affected by

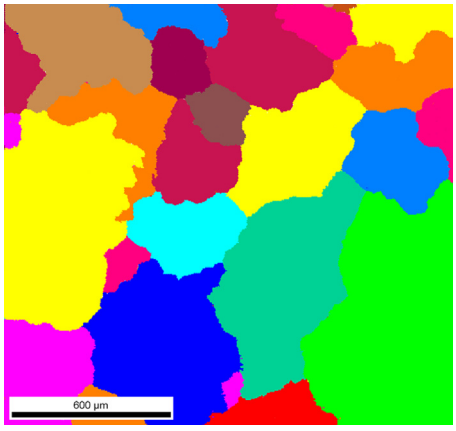

Fig. 1. Orientation imaging microscopy of 2099 alloy.